
Urban inundation models based on the Shallow Water equations. Numerical and practical issues.

Francisco Alcrudo and Jonatan Mulet

*Area Mecánica de Fluidos, CPS - Universidad de Zaragoza,
c./ María de Luna 3, 50.018-Zaragoza, Spain
Email: alcrudo@unizar.es, jmulet@unizar.es*

ABSTRACT. A flood propagation model based on the Shallow Water equations has been applied to simulate flow inside urban areas. The model is equipped with the artifacts required to accurately solve the governing equations. The mathematical description of the urban area is performed in different ways in order to find the best strategy to be applied in actual real life computations.

RÉSUMÉ. Un modèle de simulation d'inondations basé sur les équations de Saint Venant a été appliqué à des inondations en zone urbanisée. Le modèle est équipé avec les outils numériques requis pour la solution précise des équations différentielles. La modélisation mathématique de la zone urbanisée est faite de façons diverses afin de trouver la meilleure stratégie à appliquer dans des cas réels.

KEYWORDS: Shallow water equations, flood propagation, urban flooding

MOTS-CLÉS : équations de Saint Venant, propagation de crues, inondations urbaines

1. Introduction

This paper presents some of the work devoted to simulate flood propagation in real life scenarios. This usually entails the propagation of a flood wave over natural terrain (in many cases a river valley) often affecting also populated areas. Most of the work reported here has been performed within the EU IMPACT project aiming at improving our modelling capability in actual events, with special emphasis on those involving urban areas where damages can be most devastating. The model used is based upon the Shallow Water Equations (SWE), that presently constitute the most common mathematical framework for this type of studies. The SWE represent so far a good compromise between physics complexity and solvability at the scales of real

problems. More elaborate equations do not seem yet practical for routine use in real life problems because the length scale of the problem ranges in the order of Kilometers and the required resolution is several orders of magnitude smaller.

During the work reported here, special emphasis has been given to the simulation of urban flooding at a local scale, meaning by this the aim of computing local water elevation and depth averaged flow velocity amidst the streets of an urban area [HAI 01]. This is in contrast to the more common approach of simulating urban areas as regions simply characterized by higher friction, reduced conveyance, and or some sort of porosity to account for the blocking effect of buildings [TES 98]. The local approach can give in principle a more accurate description of the flood enabling a more precise planning of counter measures and risk evaluation. However it also results in a considerably higher cost, which is mainly due to the needed increase of resolution of about one order of magnitude with respect to the porosity or averaged approach.

Local description of the flow in urban regions is achieved without modifying the mathematical model which is still based upon the SWE. The presence of buildings is accounted for by introducing their effects on the shallow water model by the following techniques: a) Increasing the bed friction locally, well above normal values, to model the presence of an obstacle (building). b) Representing buildings as solid walls, what only requires a precise meshing of the urban area. c) Representing buildings as abrupt elevations of the bed function. In order to test the accuracy of the model to depict urban flooding, its output was compared with experimental and actual flooding data.

2. Governing equations

The SWE represent an approximation to the free surface flow of a fluid in a horizontal plane over a prescribed bottom surface given by a bed function $z_B(x, y)$. Denoting the depth of the fluid layer by h and the depth averaged cartesian velocity components by u and v , the 2-D SWE can be written as:

$$\frac{\partial \mathbf{U}}{\partial t} + \nabla \cdot \mathbf{F} = \mathbf{S}_b + \mathbf{S}_f \quad (1)$$

where the flux tensor, \mathbf{F} can be split in its two cartesian components:

$$\mathbf{F} = (\mathbf{E}, \mathbf{G}) \quad (2)$$

the conserved variables and flux vectors \mathbf{U} , \mathbf{E} , \mathbf{G} , are given by:

$$\mathbf{U} = \begin{bmatrix} h \\ hu \\ hv \end{bmatrix}, \quad \mathbf{E} = \begin{bmatrix} hu \\ hu^2 + gh^2/2 \\ huv \end{bmatrix}, \quad \mathbf{G} = \begin{bmatrix} hv \\ huv \\ hu^2 + gh^2/2 \end{bmatrix} \quad (3)$$

and the sources \mathbf{S}_b and \mathbf{S}_f by:

$$\mathbf{S}_b = -gh \begin{bmatrix} 0 \\ \partial z_B / \partial x \\ \partial z_B / \partial y \end{bmatrix}, \quad \mathbf{S}_f = -\frac{gn^2 \sqrt{u^2 + v^2}}{h^{1/3}} \begin{bmatrix} 0 \\ u \\ v \end{bmatrix} \quad (4)$$

where the empirical Manning's formula has been used to express the bed friction slope. In the form written above, the SWE embody the conservation of mass and momentum of the water layer. In the steady state, energy conservation along a streamline is also a property of the SWE system as long as there is no friction nor hydraulic jumps:

$$\frac{\partial H}{\partial t} + \mathbf{v} \cdot \mathbf{grad}H = g \frac{\partial h}{\partial t} \quad (5)$$

where H is the head:

$$H = \frac{1}{2} \mathbf{v} \cdot \mathbf{v} + g\zeta \quad (6)$$

and ζ the free surface:

$$\zeta = h + z_B \quad (7)$$

In 1-D the momentum and energy conservation equations are totally equivalent as long as the solution is smooth.

3. Numerical method

There are many methods in use today for the solution of the SWE as applied to flooding problems. There are some properties a numerical method should possess in order to be a good flood propagation model engine. Among them:

- It should be conservative (in order to preserve the basic fundamental quantities, mass and momentum)
- It should be able to capture physically meaningful weak solutions (only those dissipating energy, H)
- It should be balanced in the sense of the compatibility between the flux and source term discretisations (in order to preserve steady state equilibria)
- It should be capable of dealing with dry areas and wetting-drying fronts

3.1. Basic underlying scheme

In this work we have used a classic TVD method made up of Roe's Riemann solver and MUSCL [VLR 79] extrapolation in finite volumes, coupled with two step, second order accurate, explicit time integration. Bottom slope source terms are upwinded and bed friction is computed centrally and implicitly integrated in time. The method has proven robust and accurate in many benchmarks and applications and has been implemented in structured and non-structured grids using triangles and quadrangles. After casting the SWE in integral form for control volume V_k :

$$\frac{\partial}{\partial t} \int_{V_k} \mathbf{U} dV + \oint_{S_k} \mathbf{F} \cdot \mathbf{n} dS = \int_{V_k} (\mathbf{S}_b + \mathbf{S}_f) dV \quad (8)$$

the finite volume discretisation leads to:

$$\mathbf{U}_k^{n+1/2} = \mathbf{U}_k^n - \frac{\Delta t}{2V_k} \sum_{w_k=1}^{w_k=n_k} \mathbf{F}_{w_k}^{*n} \cdot \mathbf{n}_{w_k} \Delta s_{w_k} + \frac{\Delta t}{2} \left(\mathbf{S}_{\mathbf{b}k}^{*n} + \mathbf{S}_{\mathbf{f}k}^{n+1/2} \right) \quad (9)$$

$$\mathbf{U}_k^{n+1} = \mathbf{U}_k^n - \frac{\Delta t}{V_k} \sum_{w_k=1}^{w_k=n_k} \mathbf{F}_{w_k}^{*n+1/2} \cdot \mathbf{n}_{w_k} \Delta s_{w_k} + \Delta t \left(\mathbf{S}_{\mathbf{b}k}^{*n+1/2} + \mathbf{S}_{\mathbf{f}k}^{n+1} \right) \quad (10)$$

where \mathbf{U}_k stands for the averaged value of the conserved variables over finite volume V_k (actually in 2-D it V_k is a surface area) which is enclosed by surface S_k (in 2-D this is in fact a line). S_k is decomposed into plane walls (line segments) with surface areas (lengths) Δs_{w_k} . Subindex w_k refers to the corresponding plane wall into which S_k has been subdivided. The outward pointing normal vector of w_k is \mathbf{n}_{w_k} .

Superindices n , $n + 1/2$, and $n + 1$, refer to time levels, with Δt time spacing between levels n and $n + 1$. \mathbf{F}^* stands for the numerical flux tensor and $\mathbf{S}_{\mathbf{b}}^*$ for the numerical source vector corresponding only to the bed slope.

Friction sources $\mathbf{S}_{\mathbf{f}}$ are directly evaluated from expression (4). It must be first linearized in order to avoid solving a nonlinear system, as:

$$\mathbf{S}_{\mathbf{f}k}^{n+1} \approx \mathbf{S}_{\mathbf{f}k}^n + \left[\frac{\partial \mathbf{S}_{\mathbf{f}}}{\partial \mathbf{U}} \right]_k^n (\mathbf{U}_k^{n+1} - \mathbf{U}_k^n) \quad (11)$$

The numerical flux tensor projected onto the unit normal vector to cell wall w_k can be expressed as:

$$\mathbf{F}_{w_k}^{*n} \cdot \mathbf{n}_{w_k} = \frac{1}{2} \left[(\mathbf{F}_R^n \cdot \mathbf{n})_{w_k} + (\mathbf{F}_L^n \cdot \mathbf{n})_{w_k} - |\tilde{\mathbf{A}}_{RLw_k}| (\mathbf{U}_R^n - \mathbf{U}_L^n)_{w_k} \right] \quad (12)$$

with:

$$\mathbf{F} \cdot \mathbf{n} = \mathbf{E} \mathbf{n}_x + \mathbf{G} \mathbf{n}_y \quad (13)$$

where $\mathbf{n}_{x,y}$ are the x and y components of the unit vector as usual in finite volume formulations, and:

$$\mathbf{F}_{R,L}^n = \mathbf{F}(\mathbf{U}_{R,L}^n) \quad (14)$$

$\mathbf{U}_{R,L}^n$ are suitable approximations to the value of \mathbf{U} at the right (R) and left (L) of the midpoint of cell wall w_k respectively, as dictated by the MUSCL strategy. These approximations are constructed from cell averages at adjacent cells and gradients must be limited in order to attain non-oscillatory behavior of the solution. Different interpolation schemes respecting those conditions for unstructured grids can be found in the literature [SLE 98], [HUB 99], [DAR 03]. Without loss of generality and in what follows, the left state, L , of cell wall w_k will be considered to be inside finite volume k whereas the right one, R , external to it. This is equivalent to taking a counterclockwise path for numbering the edges of the finite volume.

$|\tilde{\mathbf{A}}_{RLw_k}|$ is the matrix whose eigenvalues are the modulus of those of the Roe matrix corresponding to the normal flux and variable differences across cell wall w_k , as usual in flux difference splitting schemes:

$$(\mathbf{F}_R^n \cdot \mathbf{n})_{w_k} - (\mathbf{F}_L^n \cdot \mathbf{n})_{w_k} = \tilde{\mathbf{A}}_{RLw_k} \cdot (\mathbf{U}_R - \mathbf{U}_L)_{w_k} \quad (15)$$

In order to obtain a correct balance between the convective flux and the source term, the bed slope numerical source function takes the following expression:

$$\mathbf{s}_{\mathbf{b}k}^{*n} = \sum_{w_k=1}^{w_k=n_k} \left[\frac{1}{2} \left(\mathbf{I} - |\tilde{\mathbf{A}}_{RLw_k}| \cdot \tilde{\mathbf{A}}_{RLw_k}^{-1} \right) \cdot \tilde{\mathbf{S}}_{w_k} + \tilde{\mathbf{S}}_{Lk} \right] \quad (16)$$

In turn, the source term evaluation, $\tilde{\mathbf{S}}_{w_k}$, is performed at the Roe averaged values in order to be consistent with the compatibility between the flux and sources as follows [HUB 00]:

$$\tilde{\mathbf{S}}_{w_k} = -g \Delta s_{w_k} \frac{h_R + h_L}{2} \left(z_{B_{w_k}} - z_{B_k} \right) \begin{bmatrix} 0 \\ (\mathbf{n}_{w_k})_x \\ (\mathbf{n}_{w_k})_y \end{bmatrix} \quad (17)$$

where again subindexes L and R denote the extrapolation of h to the left (L) and right (R) of wall w_k . Recall that according to the previously stated criterion L corresponds to the inside of cell k , and R to the outside. The expression $(z_{B_{w_k}} - z_{B_k})$ corresponds to the difference between the bed elevation of the cell external (R) to wall w_k , $z_{B_{w_k}}$, and the bed elevation of the considered cell, z_{B_k} . Finally, $(\mathbf{n}_{w_k})_{x,y}$ are the x and y components of the unit normal vector external to face w_k . The last term of equation (16) reads:

$$\tilde{\mathbf{S}}_{Lk} = -g \Delta s_{w_k} \frac{h_L + h_k}{2} \left(z_{B_{w_k}} - z_{B_k} \right) \begin{bmatrix} 0 \\ (\mathbf{n}_{w_k})_x \\ (\mathbf{n}_{w_k})_y \end{bmatrix} \quad (18)$$

where h_k is the water depth at the center of cell k .

3.2. Wetting and drying

In practical applications, inundation models need to cope with wetting and drying of terrain. . Roe's Riemann solver can work at the interfaces between wet and dry cells without major difficulty in absence of friction and abrupt slopes. However, in real life situations friction and bed slope have a combined destabilizing effect that must be controlled or the calculation can be spoiled. Specific methods to solve this problem can be found in [BEN 96], [BRU 00], [HEN 00] and [QUE 02]. A simple and robust methodology based upon the definition of a threshold depth, h_o , has been used, that has been reported successful elsewhere [SLE 98], [HUB 02]. During the calculation, cells that have water depths below the threshold value ($h < h_o$) are considered as dry and their depths (and velocities) are set to zero. A search is made for dry cells that can be flooded because their bed lies below the water level of any of their neighbors and these are then wet by imposing $h = h_o$. Cell faces are then flagged as lying between wet cells or touching a dry cell. In the former case, the flow calculation is run normally. In the latter case no flux contribution will be made to any of the cells to either side of the face. Further a control on the momentum equations must be exercised

to avoid the generation of high velocities in nearly dry cells ($h > h_o$ but still $h < kh_o$ with k between 10-100). In those cells water velocity is set to zero. Since h_o is in the order of 10^{-5} - 10^{-6} m this treatment is not expected to have a significant impact on the solution.

3.3. Building representation

As mentioned before three methods have been used to include the presence of buildings in the computational model within the SWE framework. Important issues regarding the applicability of the strategies described stand their validity from a physical point of view, the ease of the implementation and set up process in real cases, and the feasibility to couple the urban area with the open field flood propagation model.

Friction based approach

The simplest option is the local friction based approach, whereby areas occupied by buildings are assigned an extremely high friction coefficient. This turns the area into a region of very low conveyance that mimics the blocking effect of a building. The value of the friction coefficient that must be prescribed to attain this blocking effect is still subject to discussion, because it appears to depend on the building size versus depth ratio and on the flow velocity. Nevertheless the friction level required shows an asymptotic behavior and choosing sufficiently high values (about two orders of magnitude those of regular roughnesses) ensure the required level of friction to model the presence of an obstacle for sufficiently high flow speeds. In practice, if using Manning's formula for the bed friction, n roughness values above 1 produce the required effect in all cases considered.

The effectiveness of this strategy depends greatly on the type of flood: The blocking effect is markedly achieved for rapid flows, where a stagnation effect in front of the building appears, and the streamlines are clearly diverted. However for slow floods (low subcritical flow) the local friction method does not provide the desired results. On the other hand it is very easy to implement and the urban area is directly coupled to the open terrain flood model. Only a sufficiently fine mesh that can resolve geometrically the buildings is needed. From the point of view of the numerical integration, friction becomes strongly dominant over inertia in those areas (mesh cells) in contrast with neighboring cells where the convective or slope term drives the solution. So far an implicit time integration of the friction source discretised as given by (11) has proven sufficiently stable. Another shortcoming of this method is the artificial local storage effect due to the accumulation of stagnant water in the areas occupied by buildings.

Detailed meshing of the street pattern

The most accurate representation of the city can be obtained by careful meshing of the different streets. In this approach buildings are modelled as material (impervious) walls and hence it only entails solving the model equations in a particularly complex domain. This choice is also easy to implement in any flood modelling code because

it needs only a (substantial) meshing effort and, in principle should provide the most accurate representation of an urban flood.

Bottom elevation

In this technique buildings are included in the bed function as abrupt rises in the bottom. The bathymetric processing is in this case straightforward and can be easily automated. First a sufficiently fine grid of the urban area is generated where buildings must be well resolved. Then the bed function is risen at the locations of the buildings to their rooftop elevation. This makes the local slope around buildings to increase dramatically (above 1) what leads to a violation of the hypothesis on which the SWE are based. However the effect of such steep slopes on the flow is the generation of a stagnation region, an effect that is reproduced by the SWE if slopes are strong. Hence it is assumed that the flow pattern computed with the SWE will mimic the actual one. Further to this, steep slopes can bring about numerical instabilities. However the numerical integration presented in previous section together with the wetting-drying strategy has proven stable and robust in all the cases computed. As an advantage, this method can model building overtopping straightforwardly.

All of the approaches listed above need highly resolved meshes if the details of the city area and hence of the flow are to be captured. In practical application this usually means cell sizes on the order of 1m.

4. Applications

The methods described above have been applied to model flooding in urban like environments in order to tell the pros and cons of each strategy, as well as to find out the overall performance trends.

The first case reported here regards the simulation of urban flooding experiments carried out on a scaled down model (1:100) of an imaginary city placed in a model of a river valley [ALC 03]. The model city was made of concrete blocks of 15cm side. A flood wave enters the model river valley at its upstream end and then reaches the model city area that is inundated. Water depth history measurements were made at different positions amidst the model houses. Two different city lay outs (houses aligned and staggered with respect to the flow direction) and valley configurations, as well as several flood intensities were tested. Figure 1 (left) shows a view of the model city placed in the valley, where buildings are represented as bed elevations. In Figure 1 (right) a simulation run is shown at a time when only part of the model city has been flooded.

Figure 2 shows the plot of water depth history at two different probe positions as simulated by means of the different strategies discussed above compared to recorded observations. The comparison shows a certain advance in the simulated arrival time of the wave with respect to actual arrival time, that can be attributable to the treatment of boundary conditions. As regards the different building representation strategies all

three provide a reasonable picture of the event, with the bottom elevation technique yielding the highest water elevation and bottom friction the lowest as could be expected from the previous discussion. In all tests and simulations run all three methods provided valuable predictions within 25 percent of observations. Nevertheless laboratory experiments have proven much easier to simulate than actual floods mainly due to the reduced size and control of the various parameters involved.

The second example corresponds to an actual flood event used as a case study during IMPACT project [ALC 03b]. It corresponds to the flood wave generated after failure of Tous dam in Spain in 1982. The flood wave reached a vast populated area downstream. For the case study only the reach 5 Km downstream of the dam, including a small town named Sumacárcel was considered. Water elevation data with (rough) timing were available for the flooding of the town and were used for comparison with model output. Overall agreement was reasonable given the uncertainties associated with some case study data. Differences between computed and observed water depths inside the town were estimated between 1m and 2m. Submersion levels were on the order of 8m to 12m.

Figure 3 shows a plan view of the river reach. The town lies on the right bank after the square shaped meander. Figure 4 depicts a close up view of the town represented as bottom elevation on a fine mesh for the purposes of the simulation. The main difficulty in computing real life cases lies in the size of the problem combined with the high resolution needed to model locally the flood in the urban area. This leads to meshes either too large or strongly stretched. In the meshes used in this work the number of cells ranged around 30000. Of the different strategies previously discussed only a detailed 2D meshing of the street pattern and the bottom elevation technique proved useful in this problem.

5. Conclusions

In this work the extension of a high resolution flood propagation model to describe urban inundation by means of different techniques has been discussed. The methodology has proven robust and yields reasonably accurate predictions in model and real life problems. Further work is needed to enhance the resolution attained by this type of simulation in real life scenarios.

Acknowledgements

This work has been supported in part by EU IMPACT project (ENV1-CT-2001-37) and the Spanish government grant BFM 2000-1053.

6. References

[ALC 03] ALCRUDO F., GARCIA P., BRUFAU P., MURILLO, J, GARCIA D., MULET J.,

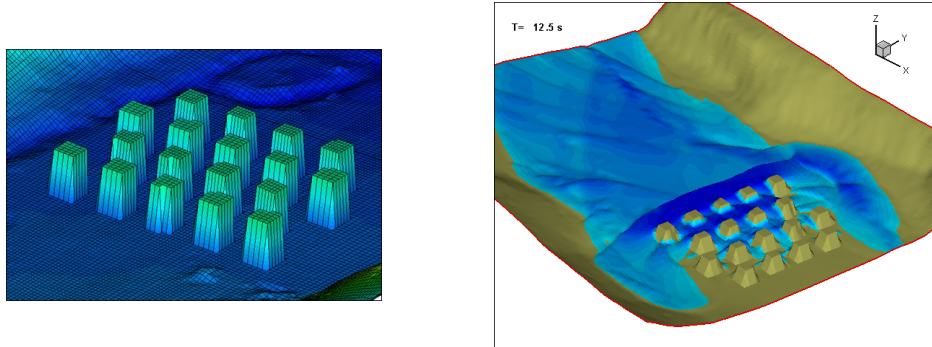


Figure 1. Model city close up and simulation run

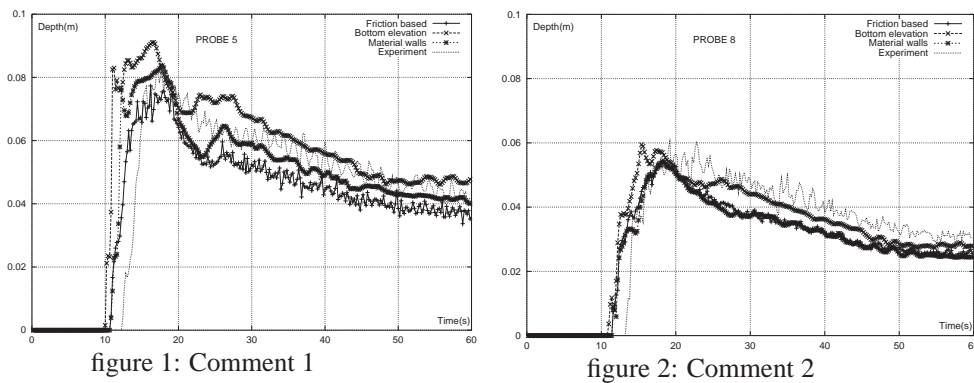


Figure 2. Simulated versus measured water depth history at two locations

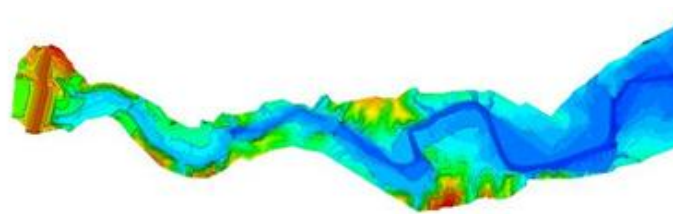


Figure 3. River valley reach considered as case study

TESTA G., ZUCCALÁ D. "The model city flooding experiment", IMPACT project internal report 2003. (www.impact-project.net).

[ALC 03b] ALCRUDO F., MULET J. "IMPACT Project Flood Propagation Case Study: The flooding of Sumacárcel after Tous Dam break". IMPACT project technical report 2003.

[BEN 96] BENTO-FRANCO A., "Modelacao computacional e experimental de escoamentos

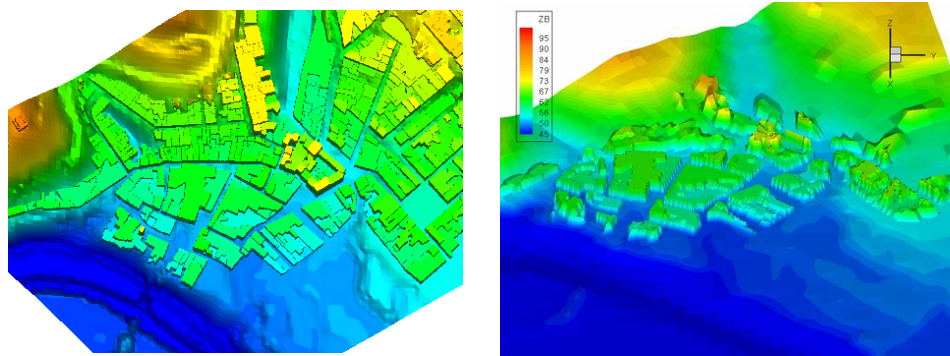


Figure 4. Case study town represented as bottom elevation

- provocados por roturas de barragens", Ph. D. Thesis, Univ. Tec. de Lisboa, Portugal, 1996.
- [BRU 00] BRUFAU P., GARCIA NAVARRO P., "2-Dimensional Dam-Break Flow Simulation", *Int. J. Num. Meth. FLuids*. 2000, Vol. 33, Iss. 1, pp.35-57.
- [DAR 03] DARWISH M.S., MOUKALLED F., "TVD schemes for unstructured grids", *Int. J. Heat & Mass Transfer*. 2003, 46, pp.599-611.
- [HAI 01] HAIDER S., "Contribution à la modélisation d'une inondation en zone urbanisée. Approche bidimensionnelle par les équations de Saint Venant", Ph. D. Thesis, INSA de Lyon, France, 2001.
- [HEN 00] HENICHE M., SECRETAN Y., BOUDREAU P., LECLERC M., "A two-dimensional finite element drying-wetting shallow water model for rivers and estuaries", *Adv. Water Res.* 2000, Vol. 23, pp.359-372.
- [HUB 99] HUBBARD M.E., "Multidimensional slope limiters for MUSCL-type finite volume schemes on unstructured grids" *Journal of Computational Physics* 1999, Vol. 155, pp.54-75.
- [HUB 00] HUBBARD M.E., GARCÍA-NAVARRO P., "Flux difference splitting and the balancing of source terms and flux gradients", *Journal of Computational Physics* 2000, Vol. 165, pp.89-125.
- [HUB 02] HUBBARD M.E., DODD N., "A 2D numerical model of wave run-up and overtopping", *Coastal Engineering* 2002, Vol. 47, pp.1-26.
- [QUE 02] QUECEDO M., PASTOR M., "A Reappraisal of Taylor-Galerkin Algorithm for Drying-Wetting Areas in Shallow-Water Computations" *Int. J. Num. Meth. Fluids* 2002, Vol. 38.
- [SLE 98] SLEIGH P.A., GASKELL P.H., BERZINS M., WRIGHT N.G., "An unstructured finite-volume algorithm for predicting flow in rivers and estuaries", *Computers & Fluids* 1998, Vol. 27, Iss. 4, pp. 479-508.
- [TES 98] TESTA, G., DI FILIPPO, A., FERRARI F., GATTI, D, "Two dimensional model for flood simulation over flat dry areas with infrastructures", *Hydroinformatics '98, Babovic and Larsen (eds.), Balkema* 1998.
- [VLR 79] VAN LEER B., "Towards the ultimate conservative difference scheme V.A second order sequel to Godunov's method", *Journal of Comp. Physics* 1979, Vol. 32, pp.101-136.